AMPTIAC

NRL Report 6805

Fatigue Crack Propagation in a High-Strength Steel Under Constant Cyclic Load with Variable Mean Loads

T. W. Crooker and E. A. Lange

Strength of Metals Branch
Metallurgy Division

November 29, 1968

NAVAL RESEARCH LABORATORY
Washington, D.C.

CONTENTS

ABSTRACT

Fatigue crack propagation studies were conducted on a 9Ni-4Co-0.25C high-strength steel using a constant cyclic load and variable mean loads. The load ratio, R, was varied from +0.5 to -1.0. Fatigue crack growth rates were analyzed using the crack tip stress-intensity factor, K. The results show that mean loads exert a strong secondary influence on fatigue crack propagation. Data were fitted to two crack propagation equations which seek to account for mean loads. Both equations significantly reduced, but did not eliminate, the "layered" scatter caused by mean loads.

PROBLEM STATUS

This report completes one phase of the problem;
work is continuing.

AUTHORIZATION

NRL Problem M01-18, Project RR 007-01-46-5420
NRL Problem M03-01, Project SF 020-01-01B-12383
NRL Problem F01-17, Project S-4607-11894

Manuscript submitted September 5, 1968.

FATIGUE CRACK PROPAGATION IN A HIGH-STRENGTH STEEL UNDER CONSTANT CYCLIC LOAD WITH VARIABLE MEAN LOADS

INTRODUCTION

The engineering approach to fatigue crack propagation has dealt largely with methods of evaluating the rate of growth of fatigue cracks. Efforts to apply linear elastic fracture mechanics to this problem were initiated by Paris and Erdogan [1], and the fracture mechanics approach to fatigue [2] has gained wide acceptance.

Extensive evidence [3] has been cited to indicate that the crack tip stress-intensity factor, K, is the primary stress parameter in controlling fatigue crack growth. Paris' equation (1) for fatigue crack growth rates employs the stress-intensity factor range, ΔK, as the primary variable in causing fatigue crack growth.

$$\frac{da}{dN} = C_1 (\Delta K)^{m_1} \qquad (1)$$

Forman, et. al., [4] have proposed a modification of Paris' equation (2) to take into account the effect of mean load through the load ratio (minimum load/maximum load), R, and the instability that can occur when the stress-intensity approaches the fracture toughness of the material, K_c (or K_{Ic}).

$$\frac{da}{dN} = C_2 \frac{(\Delta K)^{m_2}}{(1-R) K_c - \Delta K} \qquad (2)$$

Forman applied this equation to extensive experimental data on 7075-T6 and 2024-T3 aluminum alloys and found excellent correlation. Hudson and Scardina [5] also applied Forman's equation to a study of fatigue crack growth in 7075-T6 aluminum alloy sheet under variable load ratios and found that it gave the best fit among several equations examined.

Roberts and Erodgan [6] have dealt with the problem of mean stress on fatigue crack propagation in 2024-T3 aluminum alloy under tensile and bending loads. Based on their proposed model for fatigue crack propagation [7], they developed the following equation (3) to account for both cyclic and mean loads.

$$\frac{da}{dN} = C_3 (K_{max} \Delta K)^{m_3} \qquad (3)$$

This paper discusses the application of each of these equations to fatigue crack propagation in a 9Ni-4Co-0.25C high-strength steel using various load ratios. A previous study of this steel [8] indicated that its fatigue crack propagation characteristics were sensitive to load ratio and instability. The object of this study was to determine if a broad range of fatigue data gathered on this steel could be normalized on the basis of these equations.

MATERIAL

The material under investigation is a 9Ni-4Co-0.25C high-alloy commercial production steel, quenched and tempered to a yield strength of 180 ksi. This steel was processed by a special melting practice involving vacuum-carbon-deoxidation of an electric furnace air-melt heat, followed by a vacuum-consumable-electrode-remelt. Test specimens were machined from 1-in.-thick plate stock which had been evenly cross-rolled to minimize mechanical anisotropy.

The material under investigation was studied in the as-received condition which consisted of the following mill heat treatment:

1) normalize at 1600°F for one hour

2) austenitize at 1500°F for one hour, followed by an oil quench

3) temper at 1000°F with air cooling

The grain size of this material is No. 8 and finer, while R_c hardness in the plane of the fracture path is 42.

The chemical composition of this steel is given in Table 1, the mechanical properties are given in Table 2, and fracture mechanics data are given in Table 3.

EXPERIMENTAL PROCEDURE

Fatigue crack propagation tests were performed using single-edge-notched (SEN) specimens cycled in cantilever bending. The fatigue specimen is shown in Fig. 1. The

Table 1
Chemical Composition

Element	C	Mn	Si	P	S	Ni	Cr	Mo	Co	V
WT.-%	0.25	0.28	0.01	0.006	0.008	8.31	0.40	0.48	3.78	0.11

Table 2
Mechanical Properties

Specimen Orientation	0.505-in. diam. Tension Test Data				Charpy-V Energy 30°F (ft-lb)	1-in. Dynamic Tear Test Energy 30°F (ft-lb)
	0.2% YS (ksi)	UTS (ksi)	Elong. in 2-in. (%)	Red. of Area (%)		
RW*	183.2	195.0	17.0	61.0	40	1996
WR*	–	–	–	–	38	–

Table 3
Fracture Mechanics Data

Specimen Orientation	Type of Specimen	No. of Tests	Average Corrected K_{Ic}** (ksi $\sqrt{in.}$)	K_{Iscc}*** (ksi $\sqrt{in.}$)	NRL Investigator
RW*	Sen Tension	2	155	–	C.N. Freed
WR*	Sen Tension	2	153	–	C.N. Freed
WT*	Bend-Bar	4	159	–	H.L. Smith
RW*	Bend-Bar	–	–	100	G. Sandoz

* Ref. 9
** Ref. 10
***Ref. 11

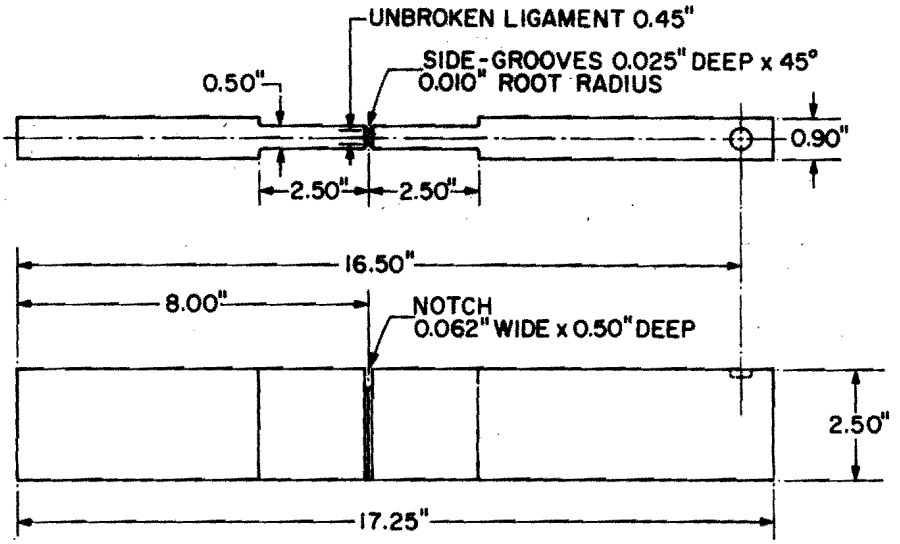

Fig. 1 - Details of the NRL single-edge-notched (SEN) cantilever fatigue specimen with side-grooves

test section has nominal dimensions of 2.5-in. wide and 0.5-in. thick. The net thickness is reduced to 0.45-in. by side-grooving, which acts to suppress shear lip formation and promote a straight crack front. The edge-notch is nominally 0.5-in. deep and fatigue crack propagation is allowed to extend the flaw to a maximum total depth of 1.5-in. Measurements of fatigue crack length are performed by a slide-mounted optical micrometer focused on the root surface of the side-groove. The combination of test section thickness and side-groove geometry employed on this specimen results in a crack front of nearly uniform depth through the thickness, i.e., a straight crack front, thereby allowing accurate measurements from surface observations.

The fatigue crack propagation tests were run under constant load at a frequency of 5 cpm. All specimens were cycled to fracture, which occurred before gross yielding. As the crack propagates through the test section, the stress-intensity factor range, ΔK, increases, thus producing a range of crack growth rates for study. The stress-intensity characteristics of the fatigue specimen are illustrated in Fig. 2, where the relationship between stress-intensity factor, K, and flaw size, a, is shown for several values of load. Flaw size is defined as total crack depth measured from the specimen edge and includes the nominal 0.5-in. deep notch. The stress-intensity curves in Fig. 2 were computed from Kies' equation [12].

All but one of the fatigue tests performed in this study employed a cyclic load range of 1500 lbs. Using the term R to denote the load ratio (minimum load/maximum load), the following load ratios were used: R = -1.0 (-1500 to +1500 lbs.), R = -0.20 (-250 to +1250 lbs.), R = 0 (0 to +1500 lbs.), R = 0.14 (+250 to +1750 lbs.), R = 0.25 (+500 to +2000 lbs.), R = 0.40 (+1000 to +2500 lbs.), and R = 0.50 (+1500 to +3000 lbs.).

RESULTS AND DISCUSSION

Results of the fatigue crack propagation tests are shown in Figs. 3 and 4, which are plots of flaw size versus cycles of repeated load. Data from the zero-to-tension (R = 0) test are used as the reference curve in both figures. Fig. 3 shows data from the tension-to-tension (R > 0) tests, and Fig. 4 shows data from the tension-to-compression (R < 0) tests. Stress-intensity factors are calculated from various

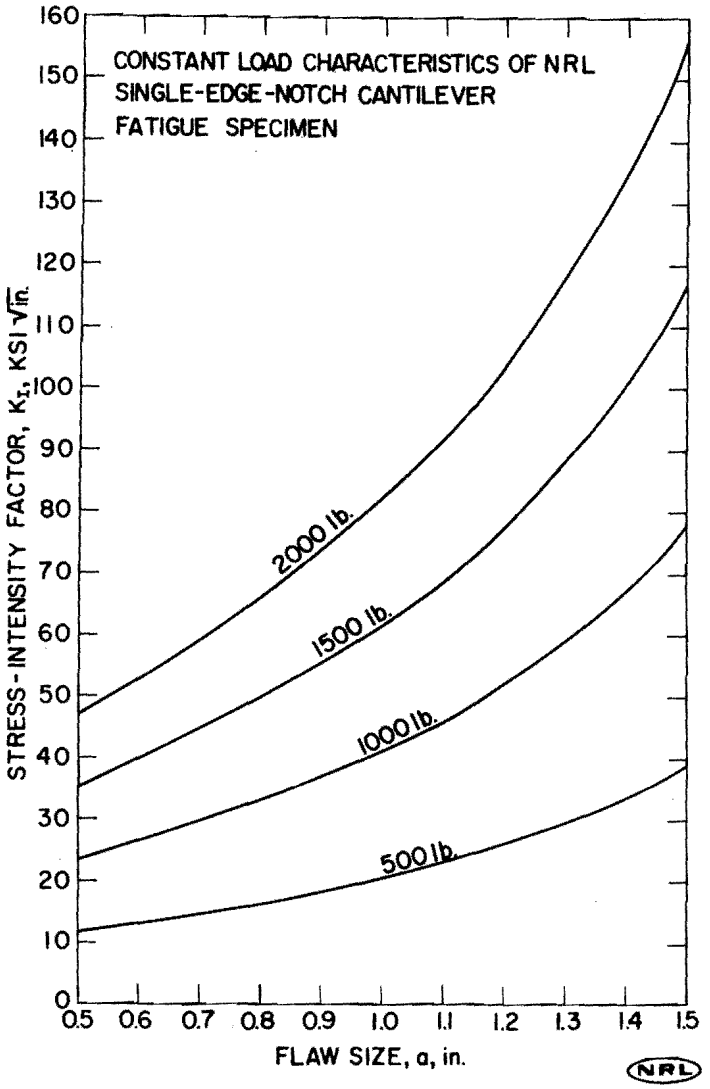

Fig. 2 - Stress-intensity characteristics of the SEN fatigue specimen as a function of flaw depth for various loads. The curves were calculated from Kies' equation, Ref. 12

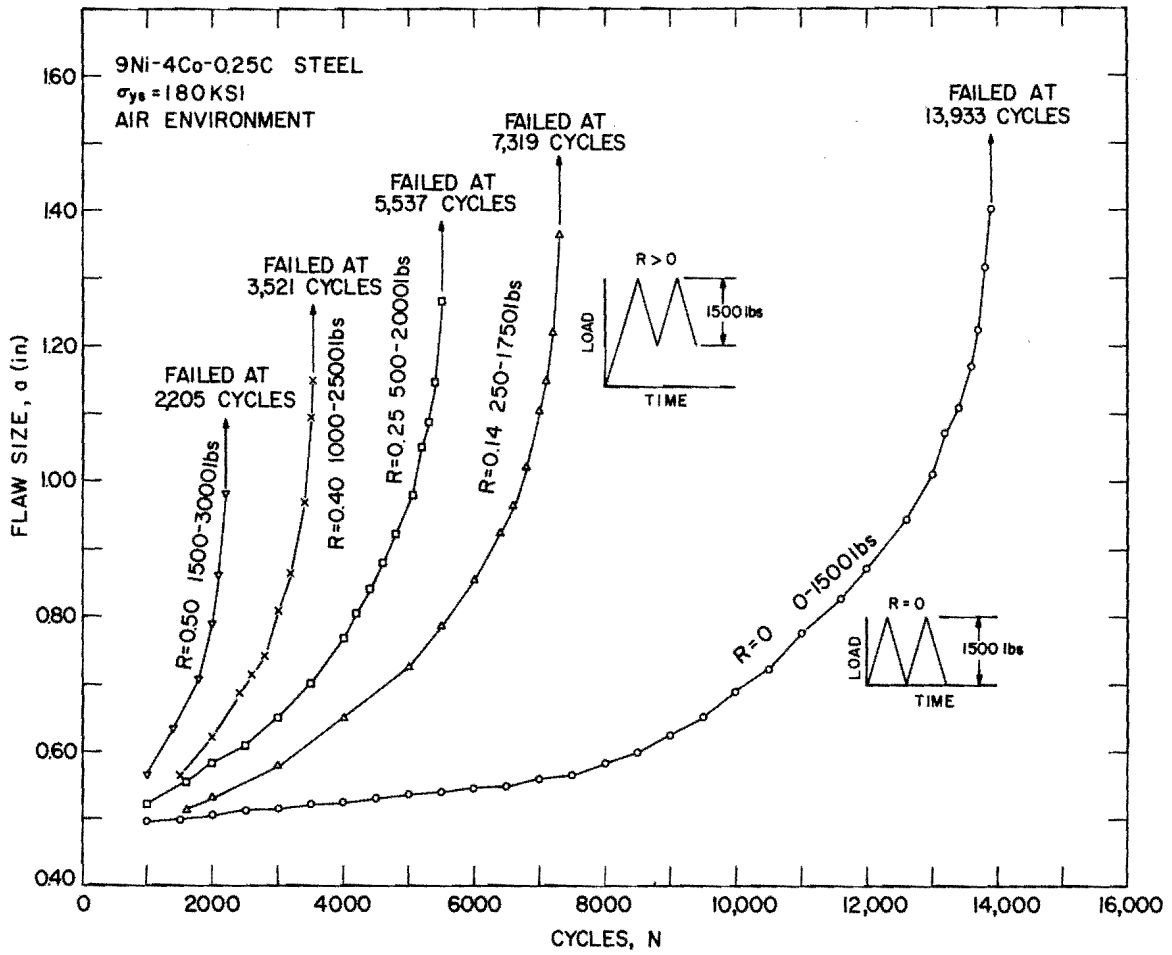

Fig. 3 - Fatigue crack propagation data for specimens cycled zero-to-tension (R = 0) and tension-to-tension (R < 0)

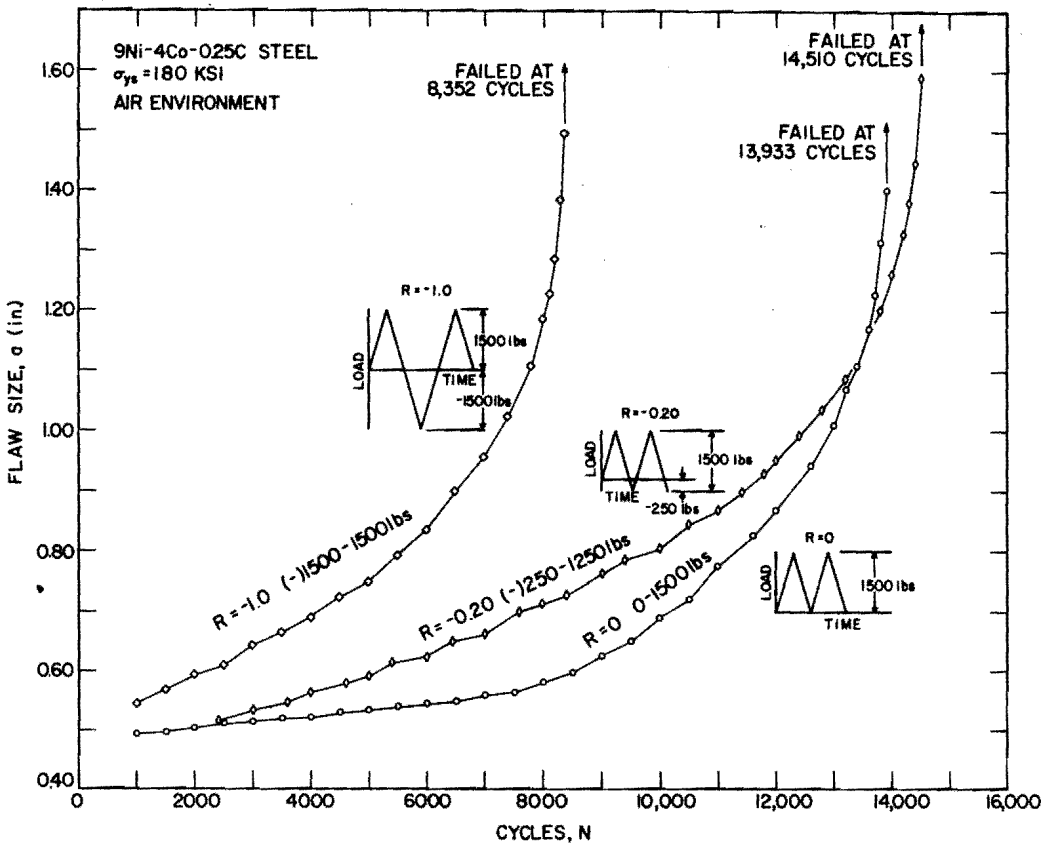

Fig. 4 - Fatigue crack propagation data for specimens cycled zero-to-tension (R = 0) and tension-to-compression ($R_{|} > 0$)

selected flaw sizes, the load, and the specimen geometry; the corresponding fatigue crack growth rates are the slopes of the curves at the selected points. Fatigue crack growth rate data are plotted as a function of stress-intensity factor range on log-log coordinates in Fig. 5. Calculations for stress-intensity values in fatigue did not include a plastic zone size correction [3]. However, the K_{Ic} values reported in Table 3 are corrected for plasticity.

The data shown in Fig. 3 indicate that tensile mean loads exert a twofold influence on fatigue crack propagation. First, crack growth rates increase with increasing tensile mean loads, even though the cyclic load remains constant. Second, the critical flaw size for fracture decreases with increasing tensile mean load, because terminal fracture is determined by the maximum stress-intensity factor value. These two combined effects are reflected in the reduction in the number of cycles to failure and in the flaw sizes attained in Fig. 3 for various specimens with increasing load ratios.

The effect of tensile mean loads on crack growth rates is shown in quantitative terms in Fig. 5. The crack growth rate data in Fig. 5 are distinctly "layered"; i.e., data points are separated on the basis of load ratio with the higher R values occupying the upper limits of the scatter. In terms of Paris' equation (1), both the material constant C_1, and the power exponent m_1, appear to increase with increasing R values. A fourth power slope is indicated on Fig. 5 for reference purposes, as it closely approximates the slope of much of the data. However, at higher ΔK values and/or higher R values, the data follows slopes greater than 4:1. Fig. 5 shows that for the 1500 lb. cyclic load employed, crack growth rates in the material under investigation can vary by as much as an order of magnitude in response to varying tensile mean loads.

Fig. 4 shows that compressive loads also exerted a significant effect on fatigue crack propagation. However, these effects occurred mainly in the early stages of the tests and are not as clearly reflected in the data shown in Fig. 5. One possible explanation for this is that, as the crack tip process zone propagates into the specimen, the constant compressive load applied in bending exerts a diminishing influence as the crack tip approaches the

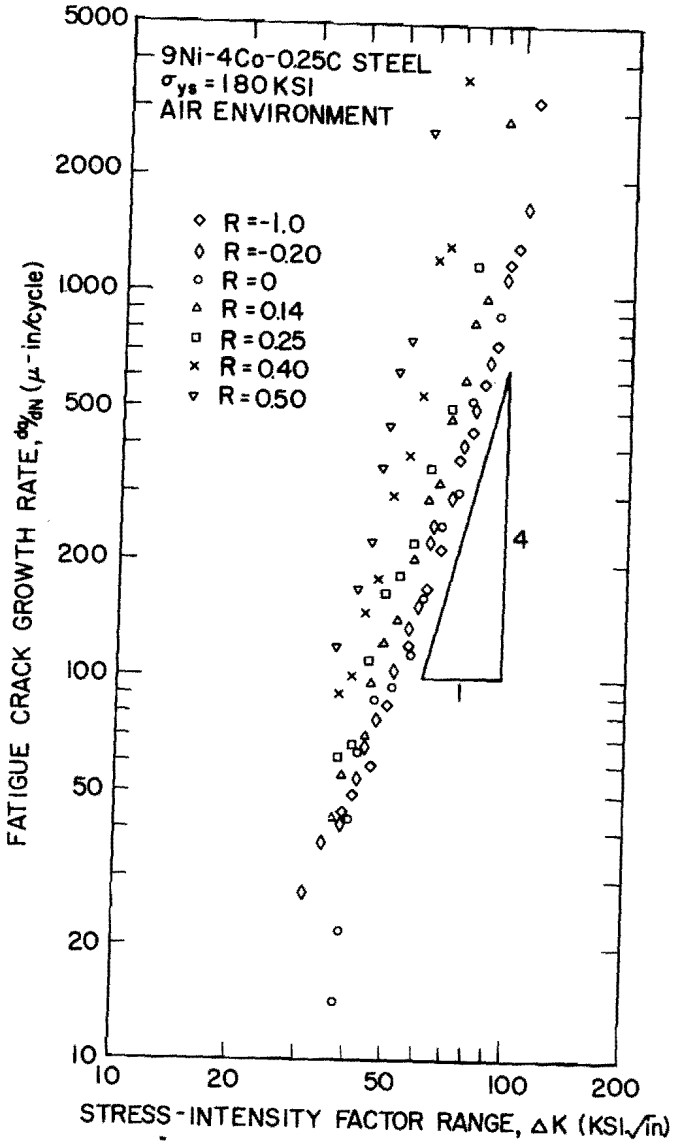

Fig. 5 - Log-log plot of fatigue crack growth rate, da/dN, as a function of stress-intensity factor range, ΔK, Ref. 1

neutral bending axis. Therefore, the effects of compressive loading are reflected most clearly by the relative number of cycles to failure for the specimens plotted in Fig. 4, as compared with the zero-to-tension (R = 0) reference curve.

For the two specimens cycled tension-to-compression (R = -1.0 and R = -0.20), only the tensile portion of the load range was used to compute stress-intensity factor values; i.e., compressive loading was ignored. This procedure was also followed in all subsequent calculations. Crack growth rate data from these tests coincide with data from the zero-to-tension (R = 0) test in Fig. 5, indicating that the compressive loading had no effect on crack propagation. This is in agreement with the conclusions reached by Hudson and Scardina [5] and other researchers [13]. However, the experimental data given in Fig. 4 suggest that this probably is not universally true, and that there is more to be learned about the effects of compressive loading on fatigue crack propagation.

In view of the scatter amongst the crack propagation data in Fig. 5, it was decided to attempt to fit these data to more complex crack propagation equations, which seek to account for mean loads as well as cyclic loads. Two such equations were chosen, the equation by Forman, et. al., (2) and the equation by Roberts and Erdogan (3). The results of these efforts are shown in Figs. 6 and 7, respectively.

The Forman equation is more complex and required more experimentation to determine the exponent value. For aluminum alloys [4], Forman found that $m_2 = 3$ provided the best fit for equation (2). Computerized computations using exponent values 2.0, 2.5, 3.0, 3.5, and 4.0 revealed $m_2 = 3$ also provided the best fit for the steel under investigation in this study. K_{Ic} for this material has been extensively investigated as reported in Table 3. A value of 150 ksi$\sqrt{\text{in.}}$ was employed for computations involving equation 2. No negative R values were used in computations; R = 0 was substituted instead, as previously discussed.

The results of the data treated according to the Forman equation are shown plotted on log-log coordinates in Fig. 6. The scatter and "layering" of the data are not completely eliminated, but are reduced considerably from that in Fig. 5. The variation in crack growth rates

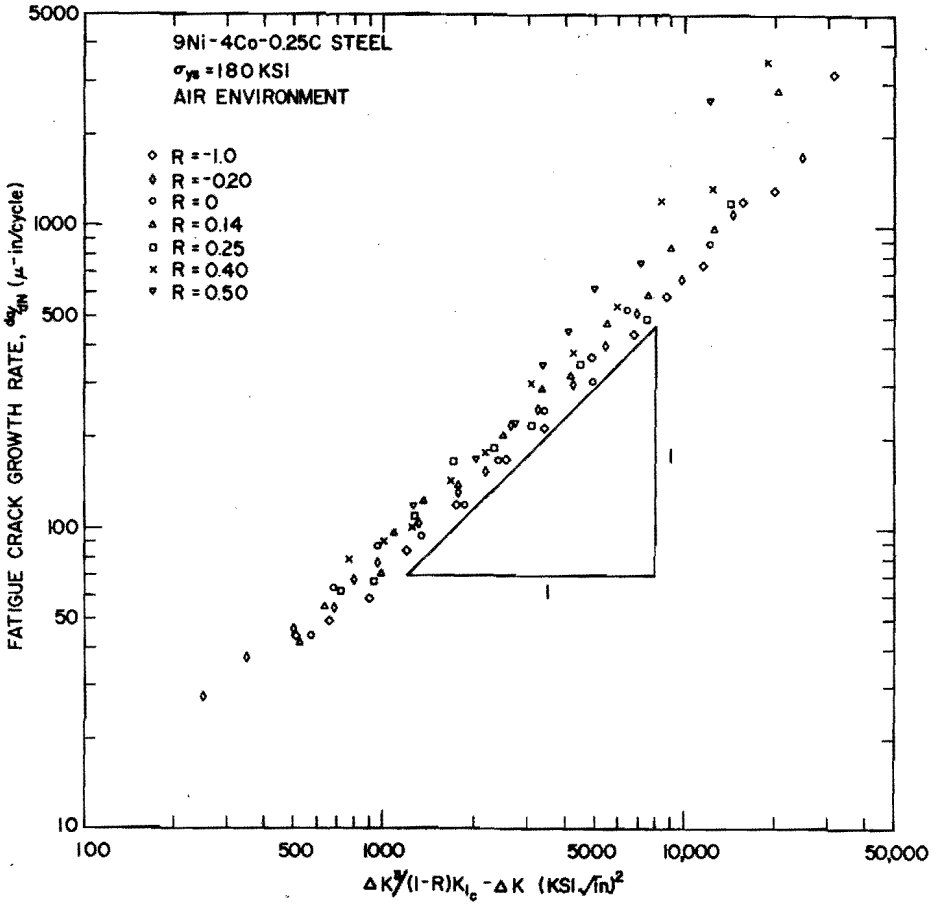

Fig. 6 - Log-log plot of da/dN as a function of $\Delta K^3/(1-R)$ $K_{Ic}-\Delta K$, Ref. 4

for any given value of the parameter, $\Delta K^3/(1 - R)K_{Ic} - \Delta K$, is approximately half as great as in Fig. 5. A 1:1 reference slope is shown in Fig. 6, and it can be seen that much of the data does vary in a linear manner with the parameter used.

Data plotted according to the equation of Roberts and Erdogan (3) are shown in Fig. 7. The scatter and "layering" amongst the data are reduced somewhat from that seen in Fig. 6, the Forman equation (2). A 2:1 reference slope is shown in Fig. 7. Much of the data does closely approximate the exponent value, $m_3 = 2$, reported by Roberts and Erdogan for 2024-T3 aluminum alloy [6].

The principal source of scatter in all of the data shown, Figs. 5-7, arises at higher values of ΔK and/or R. Such scatter is most likely caused by environmentally-assisted cracking or instability related to fracture toughness. The K_{Iscc} level of this material has been established at 100 ksi$\sqrt{in}$., Table 3. Therefore, it is conceivable that atmospheric moisture could have contributed to crack propagation rates among the upper few data points. However, an electron fractographic examination of several of the specimens [8], indicated that crack propagation at higher ΔK levels occurred exclusively by shallow dimpled rupture. These findings are more suggestive of fracture instability contributing to the scatter, rather than environmental cracking.

CONCLUSIONS

It is concluded from the study that mean loads, both tensile and compressive, exerted a significant secondary influence on fatigue crack propagation in the 9Ni-4Co-0.25C high-strength steel under investigation. Crack propagation equations based on fracture mechanics concepts, which included both cyclic load and mean load parameters, were effective in analyzing fatigue crack growth rate data. Equations developed by Forman, et. al., and Roberts and Erdogan appear to offer promising analyses and deserve further examination.

ACKNOWLEDGEMENTS

The authors wish to acknowledge the work of Mr. R.J. Hicks who performed the experimental work. The authors are also grateful to the Office of Naval Research, the Naval Ship Systems Command and the Deep Submergence Systems Project for their financial support of this work.

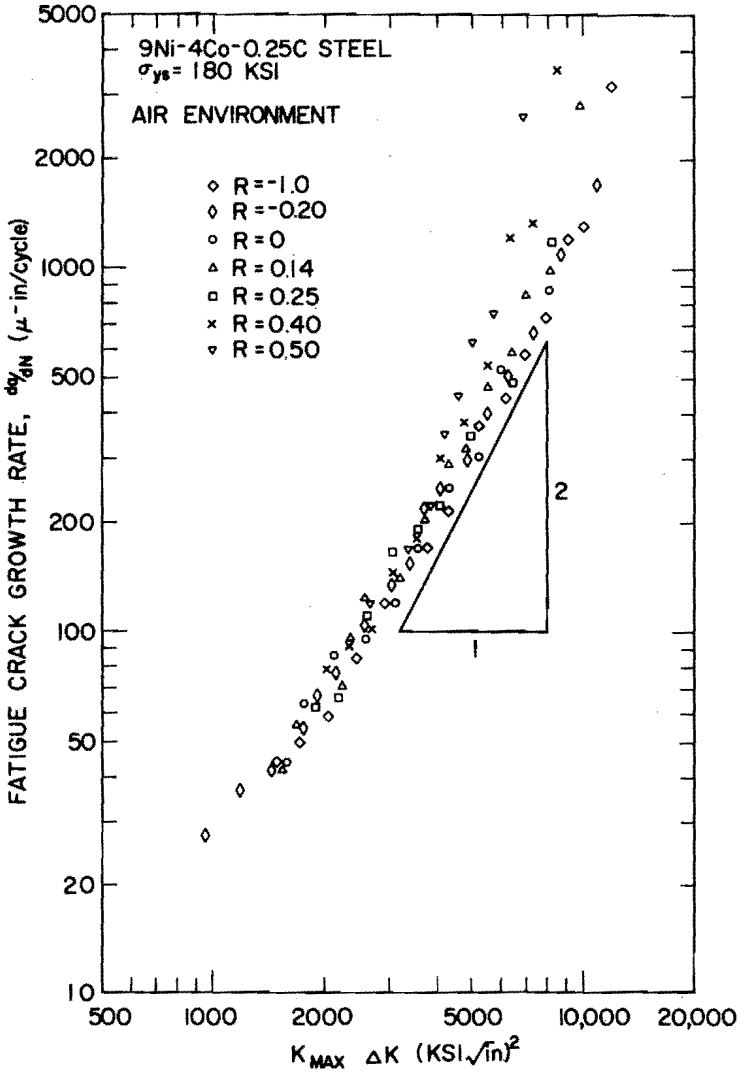

Fig. 7 - Log-log plot of da/dN as a function of (K_{max} ΔK), Ref. 6

REFERENCES

1. Paris, P. C. and Erdogan, E, "A Critical Analysis of Crack Propagation Laws," Journal of Basic Engineering, Trans. ASME, Series D, Vol. 85, 1963, p. 528

2. Paris, P. C., "The Fracture Mechanics Approach to Fatigue," Fatigue - An Interdisciplinary Approach, Proceedings Tenth Sagamore Army Materials Research Conference, 13-16 August 1963, (Syracuse University Press, 1964), p. 107

3. Johnson, H. H. and Paris, P. C., "Sub-Critical Flaw Growth," Engineering Fracture Mechanics, Vol. 1, No. 1, June 1968, p. 3

4. Forman, R. G.; Kearney, V. E.; and Engle, R. M., "Numerical Analysis of Crack Propagation in Cyclic-Loaded Structures," ASME Paper No. 66-WA/Met-4

5. Hudson, C. M. and Scardina, J. T., "Effect of Stress Ratio on Fatigue-Crack Growth in 7075-T6 Aluminum Alloy Sheet," National Symposium on Fracture Mechanics, Bethlehem, Pennsylvania, 19-21 June 1967

6. Roberts, R. and Erdogan, F., "The Effect of Mean Stress on Fatigue Crack Propagation in Plates Under Extension and Bending," ASME Paper No. 67-WA/Met-2

7. Erdogan, F. and Roberts, R., "A Comparative Study of Crack Propagation in Plates Under Extension and Bending," Proceedings of the First International Conference on Fracture, Sendai, Japan, 12-17 September 1965, Vol. 1, p. 341

8. Crooker, T. W.; Cooley, L. A.; Lange, E. A.; and Freed, C. N.; "Fatigue Crack Propagation and Plane Strain Fracture Toughness Characteristics of a 9Ni-4Co-0.25C Steel," Trans. ASM, Vol. 61, No. 3, September 1968

9. Anonymous, "The Slow Growth and Rapid Propagation of Cracks," Materials Research and Standards, Vol. 1, No. 5, May 1961, p. 389

10. Brown, W. F. Jr. and Srawley, J. E., "Plane Strain Crack Toughness Testing of High Strength Metallic Materials," ASTM STP 410, American Society for Testing and Materials, 1967

11. Brown, B. F., "A New Stress-Corrosion Cracking Test for High-Strength Alloys," Materials Research and Standards, Vol. 6, No. 3, March 1966, p. 129

12. Kies, J. A.; Smith, H. L.; Romine, H. E.; and Bernstein, H., "Fracture Testing of Weldments," Fracture Toughness Testing and Its Applications, ASTM STP 381, American Society for Testing and Materials, 1965, p. 328

13. Paris, P. C., private communication

NOMENCLATURE

a = flaw depth (machined notch plus fatigue crack)

m_1, m_2, m_3 = numerical exponents

C_1, C_2, C_3 = material constants

K = fracture mechanics stress-intensity factor

ΔK = stress-intensity factor range (maximum K minus minimum K)

K_{max} = maximum stress-intensity factor

K_c = critical stress-intensity factor for fracture (fracture toughness)

K_{Ic} = critical stress-intensity factor for initial crack instability in plane strain (plane strain fracture toughness), Ref. 10

K_{Iscc} = threshold stress intensity factor for stress-corrosion cracking in plane strain, Ref. 11

R = load ratio (minimum load: maximum load)

$\frac{da}{dN}$ = crack extension per cycle of load (fatigue crack growth rate)

Security Classification

DOCUMENT CONTROL DATA - R & D

(Security classification of title, body of abstract and indexing annotation must be entered when the overall report is classified)

1. ORIGINATING ACTIVITY *(Corporate author)*

Naval Research Laboratory
Washington, D. C. 20390

2a. REPORT SECURITY CLASSIFICATION

Unclassified

2b. GROUP

3. REPORT TITLE

FATIGUE CRACK PROPAGATION IN A HIGH-STRENGTH STEEL UNDER CONSTANT CYCLIC LOAD WITH VARIABLE MEAN LOADS

4. DESCRIPTIVE NOTES *(Type of report and inclusive dates)*

A final report on one phase of the problem; work is continuing on other phases.

5. AUTHOR(S) *(First name, middle initial, last name)*

T. W. Crooker and E. A. Lange

6. REPORT DATE	7a. TOTAL NO. OF PAGES	7b. NO. OF REFS
November 29, 1968	22	12

8a. CONTRACT OR GRANT NO.	9a. ORIGINATOR'S REPORT NUMBER(S)
NRL Problem M01-18, M03-01, and b. PROJECT NO. F01-17 Projects RR 007-01-46-5420, SF 020-01- c. 01B-12383, and S-4607-11894 d.	NRL Report 6805 9b. OTHER REPORT NO(S) *(Any other numbers that may be assigned this report)*

10. DISTRIBUTION STATEMENT

This document has been approved for public release and sale; its distribution is unlimited.

11. SUPPLEMENTARY NOTES	12. SPONSORING MILITARY ACTIVITY
	Department of the Navy (Office of Naval Research, and Naval Ship Systems Command) Washington, D.C. 20360.

13. ABSTRACT

Fatigue crack propagation studies were conducted on a 9Ni-4Co-0.25C high-strength steel using a constant cyclic load and variable mean loads. The load ratio, R, was varied from +0.5 to -1.0. Fatigue crack growth rates were analyzed using the crack tip stress-intensity factor, K. The results show that mean loads exert a strong secondary influence on fatigue crack propagation. Data were fitted to two crack propagation equations which seek to account for mean loads. Both equations significantly reduced, but did not eliminate, the "layered" scatter caused by mean loads.

DD FORM 1 NOV 68 1473 (PAGE 1)

S/N 0101-807-6801

Security Classification

14. KEY WORDS	LINK A		LINK B		LINK C	
	ROLE	WT	ROLE	WT	ROLE	WT
Fatigue crack propagation Flaw growth High-strength steel Variable mean loads Fracture mechanics						